



HAL
open science

Porous and cracked rocks elasticity: Macroscopic poroelasticity and effective media theory

Jerome Fortin, Yves Guéguen

► **To cite this version:**

Jerome Fortin, Yves Guéguen. Porous and cracked rocks elasticity: Macroscopic poroelasticity and effective media theory. *Mathematics and Mechanics of Solids*, 2021, 10.1177/10812865211022034 . hal-03272877

HAL Id: hal-03272877

<https://hal.science/hal-03272877v1>

Submitted on 28 Jun 2021

HAL is a multi-disciplinary open access archive for the deposit and dissemination of scientific research documents, whether they are published or not. The documents may come from teaching and research institutions in France or abroad, or from public or private research centers.

L'archive ouverte pluridisciplinaire **HAL**, est destinée au dépôt et à la diffusion de documents scientifiques de niveau recherche, publiés ou non, émanant des établissements d'enseignement et de recherche français ou étrangers, des laboratoires publics ou privés.

Porous and cracked rocks elasticity: Macroscopic poroelasticity and effective media theory

Mathematics and Mechanics of Solids
1–15

© The Author(s) 2021

Article reuse guidelines:

sagepub.com/journals-permissions

DOI: 10.1177/10812865211022034

journals.sagepub.com/home/mms**Jérôme Fortin**  and **Yves Guéguen***Laboratoire de Géologie, UM4 8538, CNRS, Ecole normale supérieure, PSL University, Paris, France*

Received 25 March 2021; accepted 12 May 2021

Abstract

Macroscopic poroelasticity and effective medium theory are two independent approaches which can be used to analyze the role of pores, cracks, and fluid on elastic properties. Macroscopic poroelasticity belongs to the macroscopic framework of thermodynamics whereas effective medium theory expresses the medium properties in terms of microstructural characteristics (pore and crack shape, etc.) and component properties (fluid properties, solid grain properties, etc.). In this paper, we review the fundamental assumptions and results of both approaches, and show that they are complementary but do not apply over the same range of conditions. A compilation of data is reported, in various dry and saturated rocks, to show the validity of the Gassmann equation and the dispersion between unrelaxed modulus –where effective medium model applies- and relaxed modulus –where poroelasticity applies.

Keywords

poroelasticity, effective medium theory, frequency effects, porous and cracked rocks

1. Introduction

Sedimentary rocks are of major economic importance since they constitute the hydrocarbon natural reservoirs, and also the storage reservoirs (CO₂, hydrogen, nuclear waste, etc.). Sedimentary rocks may have porosities up to some 40% with pore sizes in the range from 10 nm to 100 μm. Pore shapes are irregular. The overall physical properties strongly depend on the pore space geometry.

Igneous rocks' porosity is usually very small. In granites, for instance, it is less than 5% and microcracks are dominant. The case of basalts is very different, however; porosities can be much higher (large pores can exist due to gas exsolution) while cracks may also be present.

Elastic waves provide the most important way to “see” the deep crustal layers and thus to get some information on the in-situ rocks. It follows that elastic properties of rocks are of key importance to investigate them. While the porosity associated with cracks is usually very small, microcracks play a major role in determining the macroscopic elastic properties of a rock. The fact that microcracks can alter the effective elastic properties of a rock substantially, in spite of their very small pore volume, was noted very early by Simmons and Brace [1] and Walsh [2]. When fluids are present, elastic properties

Corresponding author:

Jérôme Fortin, Laboratoire de Géologie, UM4 8538, CNRS, Ecole normale supérieure, PSL University, 24 rue Lhomond, 75005 Paris, France.

Email: fortin@geologie.ens.fr

are also strongly modified and some knowledge of pore volume and fluid nature can be obtained from the elastic parameters. The Gassmann equation [3] and Biot theory [4] have been much used in geophysics for that reason.

Two independent approaches are useful to analyze the role of pores and cracks on elastic properties. They are independent, and some confusion arose from the fact that this independence has not always been acknowledged. The first, sometimes called Biot theory because Biot has been a pioneer in the matter, is called “macroscopic poroelasticity” in this paper. It can be seen as a formally analog theory to “thermoelasticity.” The system exchanges fluid mass with a reservoir in the present case, whereas it exchanges heat in the case of thermoelasticity. Macroscopic poroelasticity and thermoelasticity belong to the macroscopic framework of thermodynamics. Because this framework is very powerful, general relations between elastic parameters can easily be derived, which are very useful. Note that there is another way to derive poroelasticity from a microscopic model [5, 6]. Different assumptions are used in that case. They are more complex and controversial so this is not examined here.

In this paper, we refer to what we call a “second approach” as that of effective media with the goal of calculating the elastic constants. Effective media theory has been well known for a long time in solid state physics where it has been used for many different properties such as electrical properties, magnetic properties, etc., and goes back to Maxwell. The specific interest of that second approach is to express the medium properties in terms of microstructural characteristics (pore and crack shape, etc.) and component properties (fluid properties, solid grain properties, etc.). Macroscopic thermodynamics postulate the elastic constants but cannot calculate them. The importance of effective media theory is to express these constants in terms of microstructural parameters, something that a macroscopic theory cannot achieve. A key contribution to effective properties of cracked and porous rocks is that of Kachanov [7, 8]. Both approaches are complementary, but they do not apply over the same range of conditions. Ignoring this last point is sometimes a cause of misunderstanding.

2. Poroelasticity: a macroscopic theory

2.1. Fundamental assumptions

Rocks are mixture of minerals and pores or cracks, sometimes fluid-saturated. In order to build a macroscopic thermodynamic theory, the real rock has to be “homogenized.” This is the first assumption. Any rock is heterogeneous at the microscale (that of a grain, a pore, etc.). The classical concept of the “3 Ms,” for the micro-, mini-, and macro-scale is used in any theory of homogenization. What we call a “point” in the medium at the mini-scale is indeed a representative elementary volume (REV). The real rock (all real rocks are microheterogeneous) is replaced by an average homogeneous one. This assumption is a key simplification. At the mini-scale, the rock is a continuous (equivalent) homogeneous medium so that solid mechanics and thermodynamics apply. At any “point” in this equivalent medium, the material properties are defined by an average over a REV. This implies (within this theory) that it is not possible to analyze what is going on inside a “point.” Investigating non-homogeneous systems is out of our theoretical and experimental capabilities (within the framework of macroscopic poroelasticity). Attempts to use macroscopic poroelasticity for investigating the micro-scale contradict the above key assumption.

A second basic assumption is to consider fully saturated rocks. At any “point” in this equivalent medium, fluid pressure is defined in a unique way: it is defined as the equilibrium pressure of an imagined fluid reservoir to which the REV is connected (so that each pore in the REV experiments the same fluid pressure). The REV becomes a “point.” Hence, poroelasticity is not applicable if the REV is not isobaric (exactly as thermoelasticity is not applicable if the REV is not isothermal). An isobaric state should exist within a REV both in the drained and the undrained deformation regimes. This does not imply that the pores have to be connected, as an example an isobaric state within a REV exists (in the quasi-static regime) when pores have all the same shape, orientation and spacing. This last result follows from mechanics. Note that when high-frequency waves are present and when the rock contains cracks/pores of various shapes/orientations, the various pores/cracks within a given REV do not, in general, experiment the same fluid pressure, so that poroelasticity cannot be used.

However, a third key assumption of poroelasticity is to consider rocks where all pores (and cracks) are connected. Finally, a fourth assumption excludes any chemical interaction between fluid and solid.

2.2. Basic definitions

Going back to original papers is often very useful. Yet it is not easy to go through the papers of Biot. The understanding of poroelasticity was improved a lot thanks to Rice [9, 10]. Following Rice, poroelasticity is a theory that belongs to classical macroscopic thermodynamics. Biot was a pioneer but it is better to give the name “poroelasticity” to a theory that is not identical to “Biot’s theory,” assuming that one calls “Biot theory” the papers that Biot (and collaborators) published on the topic of porous rock deformation (we restrict ourselves below to analysis of quasi-static linear isotropic isothermal poroelasticity, but this can be extended as in [11]). Very often, one calls “Biot’s theory” the collection of the whole set of Biot’s papers on the subject. The above distinction is useful because there are some points in some Biot papers that are ambiguous. Not only Rice and Cleary [9], but Biot himself (in most cases) were carefully considering homogeneous systems only. It is true, however, that in a few papers, Biot took a microscopic point of view [12] that can be, and has been, questioned. It is interesting to note that in his book, de Boer [13, p. 296] wrote that “without any foundation, Biot and Willis distribute the fluid pressure, which is equal to the pore fluid pressure, over the partial solid and fluid phases.” On the next page [13, p. 297], de Boer concludes that “the essential disadvantage of Biot model lies, however, in the fact that the corresponding theory is not developed from the fundamental axioms and principles of mechanics and thermodynamics.” This remark does not apply if one refers to “poroelasticity” in the strict thermodynamics sense as defined by Rice [10]. This is precisely why we choose to refer to “poroelasticity” in this paper and not to “Biot theory.” That, as emphasized by de Boer, does not mean that the role of Biot in this story has not been a major one.

The key point is to consider the rock as a macroscopic homogeneous thermodynamic system, submitted to an external stress σ_{ij} (it could be an isotropic pressure, P , in simple cases), saturated by a fluid of volumic mass ρ_f . The fluid variables are “ m ” and “ p ”: “ m ” is the fluid mass, per unit volume of rock in the reference state (if V_p is the total pore volume for a rock volume V_0 , $m = \rho_f V_p / V_0$); “ p ” is the fluid pressure as defined previously. More precisely, what is important is the variation of mass, so that the variable ζ is introduced instead of m : $\zeta = (m - m_0) / \rho_f^0$. The quantity ρ_f^0 is the fluid mass per unit volume in the reference state and m_0 is the value of m in the reference state. The variable v (volume of fluid per unit volume of rock V_p / V_0) is by definition equal to the porosity $\Phi = V_p / V_0$. This is true of course in the saturated case only, which is the situation that we are investigating. Two basic regimes, drained and undrained, can be easily defined. The “drained” regime is a constant “ p ” regime while the “undrained” regime is a constant “ m ” regime (equivalent to constant “ ζ ” regime). The benefit of Maxwell relations is obtained when using the appropriate thermodynamics potentials with either “ p ” or “ m ” as a main variable. Two bulk moduli are defined for the porous rock, the drained modulus K_d and the undrained modulus K_u . The first corresponds to a deformation at constant “ p ”; the second to a deformation at constant “ m ”. For a porous rock volume V , they can be written as

$$1/K_d = - (1/V)(\delta V / \delta P)_p \quad (1)$$

$$1/K_u = - (1/V)(\delta V / \delta P)_m \quad (2)$$

where P denotes the isotropic pressure. Both moduli depend on the component properties (i.e., the bulk modulus of the solid mineral K_s and that of the fluid K_f) and on the porosity Φ . Note that $m = \rho_f \Phi$. When the rock is made of different minerals (isolated pores can be considered as equivalent to mineral inclusions), K_s can be considered as an equivalent solid modulus. Poroelasticity cannot give the moduli values, nor make explicit how they can be expressed in terms of K_s and K_f . Three important remarks are that (i) only the porosity Φ and the fluid unit volume mass ρ_f are to be considered because $m (= \rho_f \Phi)$ is one of the key variables, the pore shape does not appear in m and does not matter in poroelasticity; (ii) because shear is insensitive to fluid, the shear modulus μ is unique and identical in drained or undrained deformation in poroelasticity (no chemical interaction between fluid and solid); (iii) when the rock is submitted to an identical compression on the external surface and in the pores, i.e., differential pressure $P_d = \text{constant}$, or $dP = dp$, the rock deforms “as if” there were no pores, which means that the apparent bulk modulus is K_s . Because the equivalent rock is homogeneous, this implies the following equations:

$$(1/V)(\delta V / \delta P)_{P_d} = - 1/K_s \quad (3a)$$

$$(1/V_p)(\delta V_p/\delta P)_{P_d} = -1/K_s \quad (3b)$$

Let us introduce the free elastic energy $f(\varepsilon_{ij}, \zeta)$ per unit volume of rock. In the simple case of an external isotropic stress (pressure P), one obtains

$$df = -Pd\varepsilon_{kk} + pd\zeta \quad (4)$$

Note the analogy with thermoelasticity. The term $(p d\zeta)$ is the equivalent in poroelasticity of $(s dT)$ in thermoelasticity, where T is the temperature and s the entropy/unit volume.

In addition to f , other thermodynamic potentials can be introduced from Legendre transforms, such as

$$h(\varepsilon_{kk}, p) = f - p\zeta \quad (5)$$

$$dh = -Pd\varepsilon_{kk} - \zeta dp \quad (6)$$

$$g(P, \zeta) = f + \varepsilon_{kk}P \quad (7)$$

$$dg = \varepsilon_{kk}dP + p d\zeta \quad (8)$$

This thermodynamics framework allows the use of classical Maxwell relations for partial derivatives of conjugate variables (such as P , ε_{kk} , and p , ζ respectively). Here P , p , ε_{kk} , and ζ are first partial derivatives of the above potentials, and the second crossed derivatives of the potentials are equal.

Note that, in the framework of linear poroelasticity (which is the case here), the elastic moduli are constant. This implies that K_d does not depend on p , which means that it has the same value as K_d in the dry rock (if, as assumed, there is no chemical interaction). That remark could be of interest to measure K_d or to check if there is no chemical effect.

2.3. Constitutive relations

Using the variable p for the stress–strain relations, the classical constitutive relations of linear elasticity are extended in poroelasticity [11]:

$$\sigma_{ij} = (K_d - 2\mu/3)\varepsilon_{kk}\delta_{ij} + 2\mu\varepsilon_{ij} - (bp)\delta_{ij} \text{ or, for an isotropic stress, } P = -K_d\varepsilon_{kk} + bp \quad (9)$$

where b is the Biot coefficient.

Similarly, using the variable m for the stress–strain relations, the classical constitutive relations of linear elasticity become in poroelasticity [11]:

$$\sigma_{ij} = (K_u - 2\mu/3)\varepsilon_{kk}\delta_{ij} + 2\mu\varepsilon_{ij} - (BK_u\zeta)\delta_{ij} \text{ or, for an isotropic stress, } P = -K_u\varepsilon_{kk} + BK_u\zeta \quad (10)$$

where B is the Skempton coefficient.

Both parameters, the Biot coefficient b and the Skempton coefficient B , are new parameters. They are the coefficients that control the fluid effect in the constitutive equations. From (9) and (10), one obtains

$$b = (\delta P/\delta p)_{\varepsilon_{kk}} = K_d(\delta\varepsilon_{kk}/\delta p)_P \quad (11)$$

$$B = \rho_f^0 (\delta\varepsilon_{kk}/\delta m)_P = (\rho_f^0/K_u)(\delta P/\delta m)_{\varepsilon_{kk}} \quad (12)$$

2.4. Biot coefficient

Any volume increment dV can be expressed as

$$dV = (\delta V/\delta P)_p dP + (\delta V/\delta p)_P dp$$

When applying this result at constant differential pressure, $dp = dP$, and from (3), one obtains

$$(1/V)(\delta V/\delta P)_{P_d} = -1/K_s = (1/V)(\delta V/\delta P)_p + (1/V)(\delta V/\delta p)_P \quad (13)$$

$$1/K_s = 1/K_d - (1/V)(\delta V/\delta p)_P \quad (14)$$

Using (11), the above equation becomes

$$1/K_s = 1/K_d - (\delta \varepsilon_{kk}/\delta p)_P = (1 - b)/K_d \text{ or } b = (1 - K_d/K_s) \quad (15)$$

2.5. Skempton coefficient

Using (9) and (10) together, one obtains

$$P(1 - K_u/K_d) = - (K_u/K_d)bp + BK_u\zeta \quad (16)$$

For an undrained deformation where m is constant, (16) results in

$$(\delta p/\delta P)_m = (1 - K_d/K_u)/b \quad (17)$$

However, (8) implies the following Maxwell relation:

$$(\delta p/\delta P)_m = \rho_f^0 (\delta \varepsilon_{kk}/\delta m)_P \quad (18)$$

This last quantity is B , from (12), so that

$$B = (1 - K_d/K_u)/b \quad (19)$$

From (16) one can also define the specific storage coefficient under fixed stress conditions:

$$S_\sigma = (\delta \zeta/\delta p)_P = b/(BK_d) \quad (20)$$

2.6. Fluid mass variation

Another important equation expresses the fluid mass variation $\zeta(\varepsilon_{kk}, p)$. Combining, from (6), a Maxwell relation, and (11), one obtains

$$(\delta \zeta/\delta \varepsilon_{kk})_p = (\delta P/\delta p)_{\varepsilon_{kk}} = b \quad (21)$$

This implies that $\zeta(\varepsilon_{kk}, p) = b\varepsilon_{kk} + Ap$. The constant A is obtained from the undrained case where $\zeta = 0$ and p is given by (16) and (10):

$$\zeta = b\varepsilon_{kk} + [b^2/(K_u - K_d)]p \quad (22)$$

From (22) one can define the specific storage coefficient under fixed strain conditions:

$$S_\varepsilon = (\delta \zeta/\delta p)_{\varepsilon_{kk}} = b/(BK_u) \quad (23)$$

In addition, from (21), the fluid volume change $v - v_0$ is obtained from $m = \rho_f v = \rho_f (V_p/V_0)$:

$$v - v_0 = \Delta v = \Delta m/\rho_f^0 - v_0 \Delta \rho_f/\rho_f^0 = \zeta - v_0 \Delta \rho_f/\rho_f^0 = b\varepsilon_{kk} + [b^2/(K_u - K_d) - \Phi_o/K_f]p \quad (24)$$

by noting that $\Delta \rho_f/\rho_f^0 = p/K_f$

2.7. The Gassmann equation

This is a well-known equation that can be derived from (24), in the particular case $p = P = -K_s \varepsilon_{kk}$, and $\Delta v/v_0 = \varepsilon_{kk}$, because the homogeneous rock deforms as if there were no pores:

$$v - v_0 = \Phi_o \varepsilon_{kk} = b\varepsilon_{kk} + [b^2/(K_u - K_d) - \Phi_o/K_f](-K_s \varepsilon_{kk}) \quad (25)$$

Thus, (25) becomes the Gassmann equation [3]:

$$K_u = K_d + b^2[\Phi_o/K_f + (b - \Phi_o)/K_s]^{-1} \quad (26)$$

An equivalent way to obtain the Gassmann equation is to use (24) and (3) to obtain

$$1/K_s = -1/V_p(\delta V_p/\delta p)_{(Pd)} = -V_o/V_p(\delta v/\delta p)_{(Pd)} = -1/\Phi(dv/dp)_{(Pd)}$$

with (from (24)) $(\delta v/\delta p)_{(Pd)} = -b/K_s + [b^2/(K_u - K_d) - \Phi_o/K_f]$.

Note that using (25) and (26), it is possible to derive $(dv/dp)_P$. Then using (15), one obtains

$$(\delta v/\delta p)_P = 1/K_d - (1 + \Phi_o)/K_s \quad (27)$$

In the anisotropic case, Equation (26) has been extended by Brown and Korringa [14]. An important point is the issue of homogeneity. As Rice [10] or Brown and Korringa [14] have noted, there could exist an additional bulk modulus if the system is not homogeneous. It does not exist in the macroscopic approach developed above but it can be considered using the microscopic model of Cheng [5]. The fact is that porous rocks are never perfectly homogeneous (even Fontainebleau sandstone). In general, one considers them as statistically homogeneous (this is what we have done for the rocks we have investigated). Yet all the data we obtained fit reasonably well within the macroscopic poroelastic framework. One should not forget that a basic approximation is made: one looks at the “homogenized” rock as if it was a “homogeneous” rock. However, there is no other way if one wants to benefit from the powerful results of macroscopic thermodynamics.

2.8. Formal analogy between poroelasticity and thermoelasticity

It is interesting to compare poroelasticity with thermoelasticity. Biot knew thermoelasticity. It is striking to see how similar these theories are. Because the same general relations of classical thermodynamics hold in both cases, one has similar relations between isothermal K_T and adiabatic K_S bulk moduli on the one hand and between drained K_d and undrained K_u bulk moduli on the other hand. Indeed, the two parameters “ s ” (entropy per unit volume) and “ T ” (temperature) in thermoelasticity are formally equivalent to “ m ” (fluid mass per unit volume) and “ p ” (fluid pressure) in poroelasticity. The various relations between compressibilities in both cases follow directly from Maxwell relations, using the key concept of thermodynamic potential.

3. Effective elasticity: a microscopic theory

3.1. Important basic results

Using that second approach, rock elastic properties (i.e., stiffness and compliances) are calculated in terms of microstructural characteristics. The rock is heterogeneous, down to the microscopic scale, but statistical homogeneity is assumed. The fundamental assumptions of macroscopic poroelasticity introduced in the previous section are deleted. Note that this second approach has nothing in common with the microscopic model of Cheng [5]. The goal here is to derive the elastic constants and not derive poroelasticity from a microscopic model. Furthermore, one wants to explore the behavior if the fundamental assumptions of poroelasticity are not met. In the general area of solid mechanics/materials science, effective elasticity began to attract attention in the 1950s, with classical works of Mackenzie [15], Eshelby [16], and Bristow [17] on solids with spherical pores, ellipsoidal inhomogeneities, and microcracks, respectively. In rock mechanics, problems of this kind were first addressed by Walsh [2, 18]. Theoretical investigations into the effective elastic properties of cracked solids have been reviewed by Kachanov [8, 19]. For the typically irregular microstructure of rocks, the main difficulty lies in finding a quantitative characterization of the microstructure, i.e., identifying microstructural parameters in terms of which the effective elastic properties can be expressed. Microstructural defects in the form of both cracks and pores are important, but a key finding is that the dominant influence on the effective elastic properties of rocks comes from cracks, not pores. This is demonstrated, for example, by the experimental results of Fortin et al. [20] on isotropic compaction of a porous sandstone of 25% porosity. In these experiments the porosity decreased by several per cent. As an example, Figure 1 reports a decrease of 5% as the effective pressure is increased from 110 to 180 MPa; during this loading the P wave velocity (and, thus,

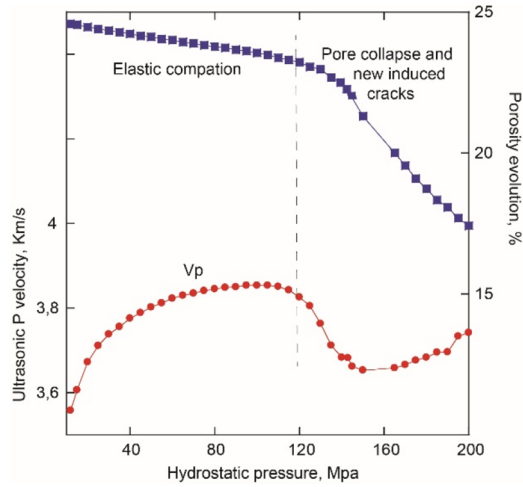


Figure 1. Porosity and P -wave velocity evolutions as a function of effective pressure in a porous sandstone (modified after Fortin et al. [20]). Pore collapse and grain crushed begin at an effective pressure of 120 MPa, leading to a porosity reduction and a decrease of the P -wave velocity.

the elastic stiffness) decreased from 3.9 to 3.65 km/s. This decrease is due to the development of new cracks. These cracks contributed to porosity in a negligible way (of the order of 0.1%), but were found to reduce the stiffness significantly whereas the porosity decrease should result in the reverse. The presence or absence of cracks of negligible volume accounts for a substantial difference in elastic properties.

Ultrasonic and seismic frequencies differ by six orders of magnitude. Frequency effects are known to exist in rocks, due mainly to the presence of fluids. At ultrasonic frequencies (10^6 Hz), fluid flow cannot “follow” the load so that the fluid pressure generally differs from pore to pore. This invalidates the fundamental local equilibrium assumption of poroelasticity theory according to which the REV is isobaric. In this case, the elastic moduli are “unrelaxed” moduli and classical poroelasticity does not apply. At lower frequencies, fluid pressure has the time to equilibrate between pores on the scale of an REV and poroelasticity applies, the elastic moduli becoming the “relaxed” moduli of poroelasticity. The critical frequency at which this local relaxation of pore pressure differences becomes effective varies in a broad range between 1 kHz and 1 MHz and depends, in particular, on the crack aspect ratio [21, 22].

3.2. Calculation of elastic moduli

In order to calculate the effective moduli, one has to start with a basis step. The REV is assumed to contain a given cavity (to be specified), and the rock is assumed to be statistically homogeneous. If an isolated cavity is placed in a solid under stress, the calculation of effective moduli has been made for simple shapes (spheres, ellipsoids). The results can be found in [23].

If there are N identical cavities in a volume V , several additional assumptions are required. The simplest one is the non-interaction approximation. In that case, the extra strain is then simply given by the sum of the contributions from all cavities. We follow this assumption in the following as it was shown to be very good for cracks. Other assumptions can be found in [23].

3.3. Cracked rocks

Because Mark Kachanov has greatly contributed to investigating cracks’ effects, and because these are of particular importance for rocks, we give more attention to that case.

For a crack, displacement of the material points on its surface S will contribute an extra strain $\Delta\varepsilon_{ij}$ to the overall strain per unit reference volume V , which is given by the surface integral over S of $(u_i n_j + n_i u_j)$ (see [8]), where u is the displacement vector generated by applied stress σ . For a flat (planar) the crack normal n is constant and $\Delta\varepsilon_{ij} = (b_i n_j + n_i b_j) S / 2V$, where $b = \langle u_+ - u_- \rangle$ is the average displacement discontinuity vector over S . This extra strain results into an extra compliance ΔS_{ijkl} to be

added to the uncracked rock compliance S^0_{ijkl} . Depending on crack orientation, the crack effect induces anisotropy.

For m cracks, each assumed to be circular with a radius a^m , Kachanov [7] introduced the second rank crack density tensor

$$\alpha_{ij} = (1/V) \sum_m (a_m^3) n_i^m n_j^m \quad (28)$$

The linear invariant $\alpha_{kk} = \rho$ is the scalar crack density, and the unique parameter in isotropic cases. The fourth rank tensor:

$$\beta_{ijkl} = (1/V) \sum_m (a_m^3) n_i^m n_j^m n_k^m n_l^m \quad (29)$$

was identified by Kachanov as a second crack density parameter. It plays a relatively minor role in dry rock or in the presence of highly compressible pore fluids in the sense that β enters in effective elastic compliances with a relatively small factor. For liquid-saturated rocks, however, the contribution to the overall elastic properties arising from the parameter β may become important so that it is a key factor for rocks saturated with water or oil.

For dry cracks, one obtains

$$\Delta S^{\text{dry}}_{ijkl} = h[1/4(\delta_{ik}\alpha_{jl} + \delta_{il}\alpha_{jk} + \delta_{jk}\alpha_{il} + \delta_{jl}\alpha_{ik}) - (v_0/2)\beta_{ijkl}]$$

Where

$$h = 32(1 - v_0^2)/3(2 - v_0)E_0 \quad (31)$$

(see [24]), where E_0 , ν_0 , and K_0 are the Young modulus, the Poisson ratio, and the bulk modulus of the matrix, respectively.

For fluid-saturated cracks, the coupling between the stress and the fluid pressure is characterized by a parameter:

$$\delta_f = 4\pi A(E_0/K_0)(1 - \nu_0^2)(K_0/K_f - 1) \quad (32)$$

It involves the average crack aspect ratio $A = w/a$ (w is the average crack aperture) as an important parameter. Clearly, δ_f will in general be different for different cracks. The parameter δ_f is zero in the limit $A \rightarrow 0$; this limit corresponds to closed cracks that are allowed to slide without friction. For a highly compressible fluid (air), $\delta_f \rightarrow \infty$; this limit recovers the case of traction-free cracks. Note that the fluid bulk modulus value K_f is constrained to be smaller than that of the solid matrix K_0 , which is indeed the situation of fluids in rocks. In the following, we assume that the values of δ_f and A are approximately the same for all cracks. The result of the calculation in that case is [24]:

$$\Delta S^{\text{sat}}_{ijkl} = h[1/4(\delta_{ik}\alpha_{jl} + \delta_{il}\alpha_{jk} + \delta_{jk}\alpha_{il} + \delta_{jl}\alpha_{ik}) - \Psi\beta_{ijkl}] \quad (33)$$

In the case of isotropy, i.e., for random crack orientations, one recovers a result of Budiansky and O'Connell [25]. We emphasize that the extra compliances ΔS_{ijkl} are the "unrelaxed" compliances (that measured at high frequencies, not that of poroelasticity). Here the tensor β is seen to enter with the multiplier:

$$\psi = [1 - (1 - \nu_0^2)\delta_f/(1 + \delta_f)] \quad (34)$$

instead of the factor $(\nu_0/2)$ for the dry case. The fact that the parameter ψ depends on the ratio K_0A/K_f of an "apparent" bulk modulus (K_0A) of the matrix to the bulk modulus of the pore fluid K_f accounts for the relative importance of the β -tensor under saturated, unrelaxed conditions.

3.4. Dispersion and attenuation due to fluids

For fluid-saturated rocks, if A is low enough so that $\delta_f \sim 0$, then $\psi \sim 1$. The results is that the difference between (29) and (26) is large. The "unrelaxed" compliances are obtained from (29) with $\psi = 1$. These are valid when the REV is not isobaric, typically at ultrasonic frequencies.

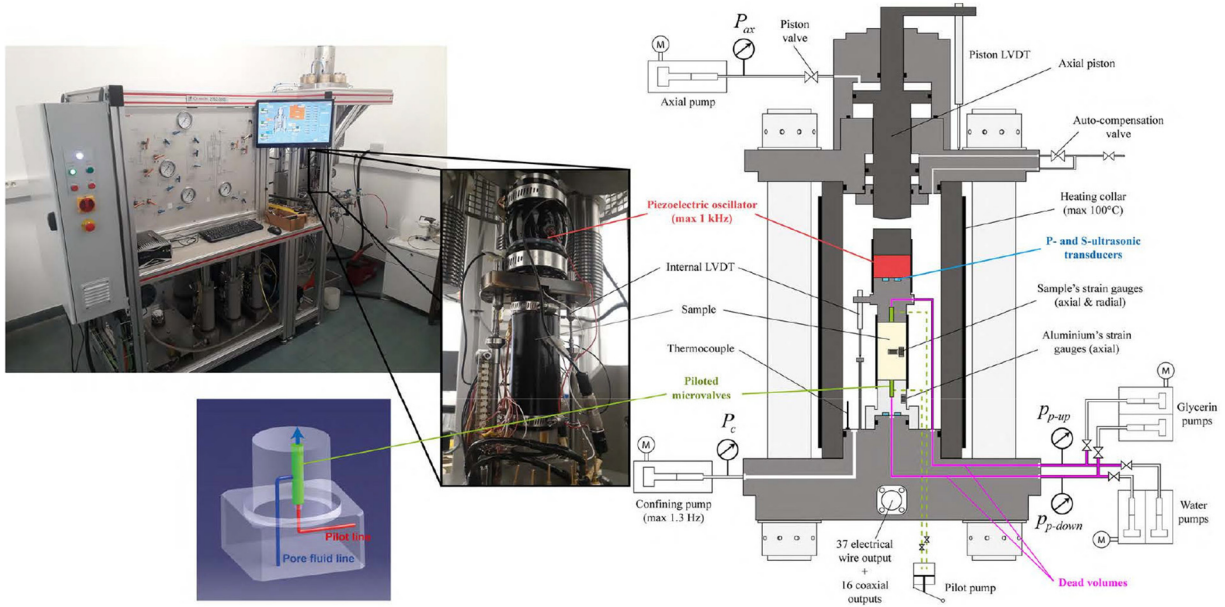


Figure 2. Experimental apparatus installed at ENS Paris. Elastic properties of a sample of 80 mm in length and 40 mm in diameter can be measured under pressure. The P and S wave ultrasonic transducers are mounted on the top and bottom end platens. Drained or undrained boundary conditions of the sample can be achieved through microvalves installed in the top and bottom end platens. Figure from Borgomano et al. [26].

On the other hand, “relaxed” compliances (i.e., undrained moduli) are obtained from the Gassmann equation (or Brown–Korringa equation in the anisotropic case) using (26). These are valid at low frequencies (typically below 1 kHz).

The dispersion (and attenuation) that results between high-frequency compliances and low-frequency compliances can be calculated from the above equations [24]:

$$S_{ijkl}^{hf} - S_{ijkl}^{lf} = h(1 - \nu_0/2)(\alpha_{ij}\alpha_{kl}/\alpha_{mm} - \beta_{ijkl})/(1 + \delta_f) \quad (35)$$

Experimental data have provided evidence of the dispersion effect in many rocks.

4. Experimental evidence

A specific apparatus (Figure 2) installed at École normale supérieure (ENS) Paris allows the measurement of (i) the elastic moduli over a broad frequency range (0.004–300 Hz) using the forced-oscillation method and (ii) the ultrasonic wave velocities P and S (1 MHz). The measurements are taken under hydrostatic pressure (0–100 MPa). Water ($K_f = 2.2$ GPa) or glycerin ($K_f = 4.36$) can be used as the pore fluid. The apparatus enables to perform two modes of stress oscillations: (i) hydrostatic, using the confining pump (range 0.004–2 Hz); (ii) axial, using a piezoelectric actuator (range 0.004–100 Hz). For hydrostatic oscillations, the confining pressure oscillates with an amplitude of about 0.2 MPa around a mean value to induce a strain oscillation amplitude in the order of 10^{-6} . The volumetric strain, ε_{kk} , is measured from strain gages and the bulk modulus is calculated as

$$K = -\Delta P/\varepsilon_{kk} \quad (36)$$

For the axial mode, a piezoelectric actuator induces axial-stress oscillations. The oscillating axial stress ($\Delta\sigma_{ax}$) is measured from axial strain gauges (ε_{alu}) glued on the lower end platen (Figure 2) made out of aluminum by $\Delta\sigma_{ax} = E_{alu}\varepsilon_{alu}$, where E_{alu} is the Young’s modulus of aluminum. Young’s modulus (E) and Poisson’s ratio (ν) of the sample can then be calculated by $E = \Delta\sigma_{ax}/\varepsilon_{ax}$ and $\nu = -\varepsilon_{rad}/\varepsilon_{ax}$, where ε_{ax} and ε_{rad} are the axial and radial strains of the sample measured by strain gauges. The bulk

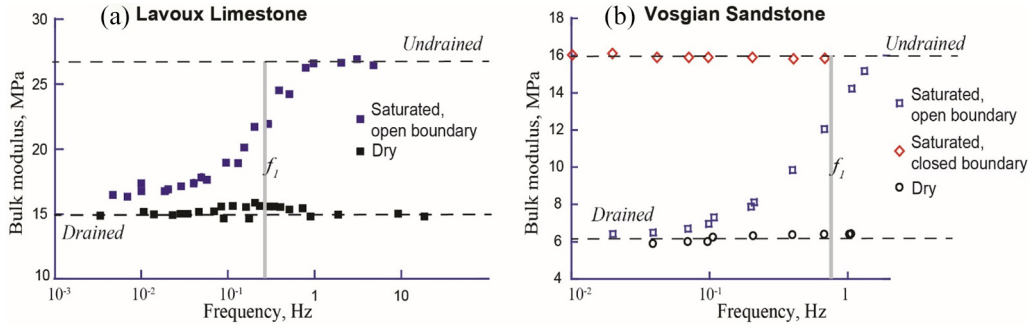


Figure 3. (a) Evolution of the bulk modulus with frequency in a Lavoux limestone in the dry and glycerin-saturated cases. The effective pressure was 2.5 MPa. (Data from Borgomano et al. [30].) (b) Evolution of the bulk modulus with frequency in a Vosgian sandstone, in the dry and glycerin-saturated cases. The effective pressure was 5 MPa. In the saturated case, open boundary and closed boundary conditions are investigated. (Data from Borgomano et al. [26].)

modulus of the sample can be deduced as $K = E/(3(1 - 2\nu))$; this last equation only holds under the assumption of elastic isotropy. One of the main advantages of the forced-oscillation method is to measure the elastic moduli under small perturbations (strain amplitude in the order of 10^{-6}) at a given pressure, as it is well known that in rocks elastic moduli varies with pressure [2, 18].

4.1. Validity of poroelasticity and the Gassmann equation

Figure 3 shows the evolution of the bulk modulus with frequency in the case of a Lavoux limestone (Figure 3(a)) and a Vosgian sandstone (Figure 3(b)). When the rock is dry (black dots), the bulk modulus is constant with frequency, as expected. When the rock is fluid-saturated, one needs to be careful with the fluid-flow boundary conditions of the sample: the cylindrical sample is jacketed, thus the lateral boundary is impermeable in terms of fluid flow. However, the top and bottom faces of the sample are connected to the pore fluid lines (Figure 2). Two cases can be considered: (1) the pore fluid is allowed to flow between the sample and pore fluid lines; (2) the fluid mass in the sample is kept constant through “closed” piloted micro-valves installed in the end pieces (green pieces on Figure 2). In this last case the dead volume induced by the microvalve is approximately $20 \mu\text{l}$ (Borgomano et al. [26]).

The evolution of the bulk modulus with frequency, in the case of open boundary condition, is shown in Figure 3 in blue dots. A clear transition can be seen from a drained regime to an undrained regime [27, 28]. The characteristic frequency for the drained–undrained transition is [29]

$$f_1 = \frac{4kK_d}{\eta L^2} \quad (37)$$

where k is the permeability, L is the length of the sample, and η is the viscosity of the pore fluid. In the case of closed boundary conditions (red dots in Figure 3(b)), the bulk modulus is constant for the frequencies investigated in this experiment and is equal to the undrained bulk modulus.

These experiments allow one (i) to measure the dry and drained bulk moduli, (ii) to check that the dry bulk modulus is equal to the drained bulk modulus, and (iii) to measure the undrained bulk modulus. Note that in the case of open boundary condition, the undrained bulk modulus can only be measured if the drained–undrained characteristic frequency, f_1 , is much lower than the relaxed–unrelaxed characteristic frequency f_2 defined in (39) (Pimienta et al. [31]). A compilation of data using this experimental approach is given in Table 1 for various sandstones and limestones.

The validity of Gassmann equation is highlighted in Figure 4. The ratio K_u/K_d on the y -axis is deduced from direct measurements (Table 1). The prediction of K_u/K_d from the Gassmann equation (26) is given on the x -axis. Overall, there is a good match between the direct measurements and the Gassmann equation, taking into account the error bar of the experimental data. One can discuss the bulk moduli of the solid mineral K_s , which is not measured in Table 1 but estimated from the mineral composition. However, according to the Gassmann equation the undrained bulk modulus is dominated

Table 1. Data compilation of dry (K_d), undrained (K_u), and high-frequency (K_{HF}) bulk moduli measured in sandstones and limestones at various effective pressures (P). The porosity is measured. The rocks are saturated by water ($K_f = 2.2$ GPa) or glycerin ($K_f = 4.36$ GPa). Here b is estimated using (15).

	ϕ	K_d (GPa)	K_u (GPa)	K_f (GPa)	K_s (GPa)	K_{HF} (GPa)	b	K_u^* (GPa)	Mineral composition	P (GPa)	Reference
Lavoux Limestone	23	15	25.9	4.36	77	25.9	0.8	25.8	100% calcite	2.5	[30]
Rustrel Limestone	14.9	13.4	30.2	4.36	77	39.9	0.82	29.3	100% calcite	2.5	[32]
	14.9	16	34.7	4.36	77	40	0.79	30.7	100% calcite	5	[32]
	14.9	20.1	35	4.36	77	40.2	0.73	33.1	100% calcite	10	[32]
	14.9	24.7	38	4.36	77	40.2	0.68	35.9	100% calcite	20	[32]
Indiana Limestone	11.4	22	31.6	2.2	77	36.8	0.71	31.6	100% calcite	2.5	[32]
	11.4	25	34.2	2.2	77	37.5	0.67	34.2	100% calcite	5	[32]
	11.4	29	37.2	2.2	77	38.3	0.62	37.2	100% calcite	10	[32]
	11.4	32.5	39	2.2	77	39	0.58	39	100% calcite	20	[32]
	11.4	22	33	4.36	77	40.2	0.71	32	100% calcite	2.5	[32]
	11.4	25	38	4.36	77	41.2	0.67	38	100% calcite	5	[32]
	11.4	29	40.6	4.36	77	41.6	0.62	40.6	100% calcite	10	[32]
	11.4	32.5	41.4	4.36	77	42	0.58	41.4	100% calcite	20	[32]
Vosgian Sandstone	24	6.2	15.7	4.36	36 ^{**}		0.8	15.8	60% qz, 30% Kfeld, 10% clay	5	[26]
Thuringen Sandstone	13	9.1	15.5	2.2	34.9 ^{**}	18.1	0.73	16.2	55% qz, 25% Kfeld, 20% clay	5	[33]
	13	10.5	17.1	2.2	34.9 ^{**}	19	0.70	16.9	55% qz, 25% Kfeld, 20% clay	10	[33]
	13	12	17.8	2.2	34.9 ^{**}	19.3	0.65	17.7	55% qz, 25% Kfeld, 20% clay	15	[33]
	13	13.7	19.1	2.2	34.9 ^{**}	19.7	0.60	18.7	55% qz, 25% Kfeld, 20% clay	20	[33]
	13	13.9	19.2	2.2	34.9 ^{**}	20	0.60	18.8	55% qz, 25% Kfeld, 20% clay	25	[33]
	13	14.5	19.7	2.2	34.9 ^{**}	20.4	0.58	19.2	55% qz, 25% Kfeld, 20% clay	30	[33]
Fontainebleau Sandstone	7	15	26.4	4.36	37.5		0.6	26.6	100% qz,	1	[31]
	7	16.8	28.8	4.36	37.5		0.55	27.2	100% qz,	2.5	[31]

* Here K_u is the prediction of the Gassmann equation (26).

** For the Thuringen and Vosgian sandstones, K_s is estimated using a Voigt–Reuss average based on the mineral composition.

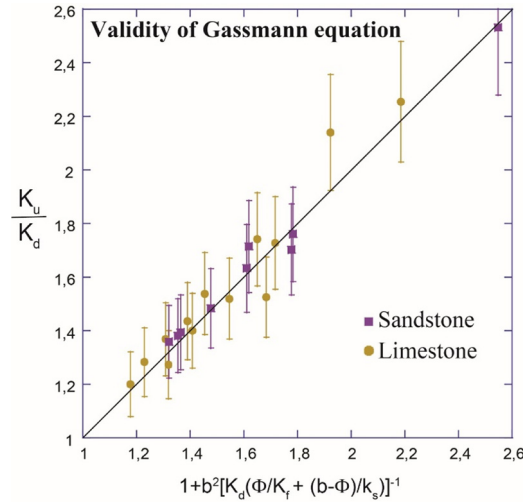


Figure 4. Measurements versus Gassmann prediction, using the data of Table 1.

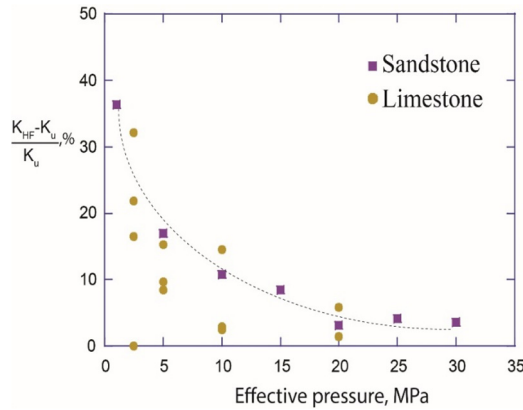


Figure 5. Dispersion between the high-frequency bulk modulus and the undrained bulk modulus (in %) versus effective pressure, using the data of Table 1.

at the first order by the value of the drained bulk modulus and the fluid bulk modulus and only at the second order by the value of K_s .

4.2. Dispersion effects due to cracks

To illustrate dispersion effects due to cracks, one can define the dispersion for a saturated rock as

$$D = \frac{K_{HF} - K_u}{K_u}, \quad (38)$$

where K_u is the undrained modulus and K_{HF} is the “high-frequency” bulk modulus deduced from ultrasonic wave velocities (frequency ~ 1 MHz). Here K_u is defined in the framework of the poroelasticity theory (relaxed state), whereas K_{HF} is an unrelaxed modulus which can be interpreted in the framework of effective medium model [8]. As shown by Adelinet et al. [34] and Fortin et al. [35], two main parameters control the dispersion, D : (i) the ratio crack porosity/total porosity and (ii) the mean crack aspect ratio. Using the data of Table 1, Figure 5 shows the evolution of the dispersion versus effective pressure

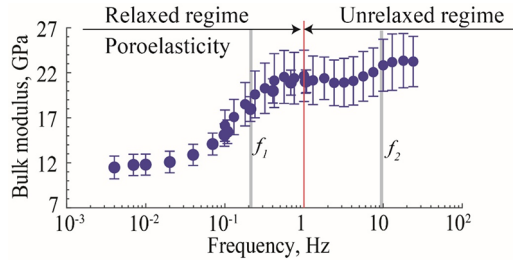


Figure 6. Evolution of the bulk modulus in a Berea sandstone saturated with glycerin at an effective pressure of 5 MPa. (Data from Chapman et al. [37].)

for various sandstones and limestones. The dispersion can reach value up to 40%, however, as shown in Figure 5, as the effective pressure increases, the dispersion decreases, as pre-existing cracks are closed.

Some rocks such as the Lavoux limestone, characterized by a bimodal porosity, show no dispersion even at low pressure [30]. Indeed, in this particular case, micro- and macro-pores have the same aspect ratio and no dispersion is expected. Another implication is to use the dispersion D (38) to distinguish between samples with or without pre-existing cracks. For example, Regnet et al. [36] measured dry and saturated ultrasonic wave velocity in microporous limestones; they estimated the undrained bulk modulus using the Gassmann equation, and computed the dispersion D to select the samples without pre-existing cracks.

Another way to observe the dispersion of elastic moduli due to cracks is to measure the elastic moduli with frequency. Figure 6 shows an example obtained on Berea sandstone [37] saturated with glycerin. Elastic modulus increases with frequency. In the relaxed regime, relevant to poroelasticity, the bulk modulus increases from the drained modulus to the undrained modulus, the characteristic frequency is $f_1 = 0.2$ Hz. Note that f_1 (36) depends on intrinsic properties of the rock (permeability, drained bulk modulus) and of the fluid (viscosity) but also on the size of sample. As the frequency increases above 1 Hz, the elastic modulus increases again from a relaxed state (where pore pressure is equilibrated at a VER scale) to an unrelaxed state (where each inclusion is individually undrained, i.e., the pore pressure inside the inclusion will mainly depends on its shape). The unrelaxed state is relevant of effective medium approach and the characteristic frequency f_2 is [21]

$$f_2 = \frac{K_s A^3}{\eta} \quad (39)$$

where A is the crack aspect ratio and η is the fluid viscosity. The characteristic frequency f_2 depends only on intrinsic properties of the rocks and the fluid. For the case of Berea sandstone (Figure 6), $f_2 = 10$ Hz, $\eta = 1 \text{ Pa}\cdot\text{s}^{-1}$, which give a mean crack aspect ratio of $\sim 10^{-3}$. Note that characteristic frequency f_2 can be rescaled for water as a pore fluid: with water as a pore fluid, the characteristic frequency is $10\text{Hz} \frac{\eta_{\text{glycerin}}}{\eta_{\text{water}}} = 10\text{kHz}$, which correspond to sonic measurements. This implies that one needs to be careful when interpreting sonic measurements with the Gassmann equation, as this last equation only holds in the relaxed regime.

5. Conclusions


Macroscopic poroelasticity and effective medium theory are two independent approaches which can be used to analyze the role of pores, cracks, and fluid on elastic properties. Macroscopic poroelasticity belongs to the macroscopic framework of thermodynamics and can be used to define the drained and undrained moduli. In this framework, one can deduce the Gassmann equation, which gives a good estimation of the seismic velocity in saturated rocks from the dry measurement, the total porosity, and the fluid bulk modulus. Effective medium theory expresses the medium properties in terms of microstructural characteristics (pore and crack shape, etc.) and component properties (fluid properties, solid grain properties, etc.). Effective medium theory can be used for fluid-saturated rocks and applies when each

inclusion is individually undrained; this is an unrelaxed state. Experimental results show (i) the validity of the Gassmann equation and (ii) that the dispersion between an unrelaxed modulus and a relaxed modulus can reach up to 40%. The dispersion is interpreted as a squirt flow from crack to pore, and the dispersion decreases as the effective pressure is increased, i.e., as pre-existing cracks are closed. The frequency characteristic between the relaxed and unrelaxed states often occurs at log frequency, which implies that the use of the Gassmann equation for sonic measurement needs to be done with caution.

Funding

This research received no specific grant from any funding agency in the public, commercial, or not-for-profit sectors. The experimental work was partially supported by the Region Ile-de-France in the framework of DIM Oxymore.

ORCID iD

Jérôme Fortin  <https://orcid.org/0000-0002-6341-3318>

References

1. Simmons, G, and Brace, WF. Comparison of static and dynamic measurements of compressibility of rocks. *J Geophys Res* 1965; 70: 5649–5656.
2. Walsh, JB. The effect of cracks on the compressibility of rocks. *J Geophys Res* 1965; 70: 381–389.
3. Gassmann, F. Elasticity of porous media. *Vierteljahrsschr der Naturforschenden Gessellschaft* 1951; 96: 1–23.
4. Biot, MA. General solutions of the equations of elasticity and consolidation for a porous material. *J Appl Mech* 1956; 78: 91–96.
5. Cheng, AHD. *Poroelasticity*. Berlin: Springer, 2016.
6. Sevostianov, I. Gassmann equation and replacement relations in micromechanics: A review. *Int J Eng Sci* 2020; 154: 103344.
7. Kachanov, M. Continuum model of medium with cracks. *J Eng Mech Div ASCE* 1980; 106(EM5): 1039–1051.
8. Kachanov, M. Effective elastic properties of cracked solids: Critical review of some basic concepts. *Appl Mech Rev* 1992; 45(8): 304–335.
9. Rice, JR, and Cleary, MP. Some basic stress diffusion solutions for fluid-saturated elastic porous media with compressible constituents. *Rev Geophys* 1976; 14(2): 227–241.
10. Rice, JR. The mechanics of earthquake rupture. In: Boeschi, E (ed.) *Proceedings of the International School of Physics Enrico Fermi, course LXXVIII on Physics of the Earth's Interior*. Amsterdam: North Holland, 1980, pp. 555–649.
11. Guéguen, Y, Dormieux, L, and Boutéca, M. Fundamentals of poromechanics. In: Guéguen, Y, and Boutéca, M (eds.), *Mechanics of Fluid Saturated Rocks*. Boston, MA: Academic Press, 2004, pp. 1–54.
12. Biot, MA, and Willis, DG. The elastic coefficients of the theory of consolidation. *J Appl Mech, ASME* 1957; 24: 594–601.
13. de Boer, R. *Theory of Porous Media*. Berlin: Springer, 2000.
14. Brown, RJS, and Korrington, J. On the dependence of the elastic properties of porous rock on the compressibility of the pore fluid. *Geophysics* 1974; 40: 608–616.
15. Mackenzie, JK. The elastic constants of solids containing spherical holes. *Proc R Soc Lond* 1950; 63B: 2–11.
16. Eshelby, JD. The determination of the elastic field of an ellipsoidal inclusion and related problems. *Proc R Soc Lond A* 1957; 241: 376–396.
17. Bristow, JR. Microcracks and the static and dynamic constants of annealed and heavily cold-worked metals. *Br J Appl Phys* 1960; 11: 81–85.
18. Walsh, JB. The effect of cracks on uniaxial compression of rocks. *J Geophys Res* 1965; 70, 399–411.
19. Kachanov, M. Elastic solids with many cracks and related problems. In: *Advances in Applied Mechanics*, Hutchinson, J, and Wu, T (eds.). London: Academic Press, 1994, pp. 256–426.
20. Fortin, J, Guéguen, Y, and Schubnel, A. Effect of pore collapse and grain crushing on ultrasonic velocities and V_p/V_s . *J Geophys Res* 2007; 112: B08207.
21. O'Connell, RJ, and Budiansky, B. Viscoelastic properties of fluid-saturated cracked solids. *J Geophys Res* 1977; 82(36): 5719–5735.
22. Le Ravalec, M, and Guéguen, Y. High and low frequency elastic moduli for saturated porous/cracked rock (differential, self consistent and poroelastic theories). *Geophysics* 1996; 61: 1080–1094.
23. Mavko, G, Mukerji, T, and Dvorkin, J. *The Rock Physics Handbook: Tools for Seismic Analysis of Porous Media*. Cambridge: Cambridge University Press, 2003.
24. Guéguen, Y, and Kachanov, M. Effective elastic properties of cracked and porous rocks. In: Leroy, Y, and Lehner, F (eds.) *Mechanics of Crustal Rocks (CISM Courses and Lectures, Vol. 533)*. Berlin: Springer, 2011, pp. 73–126.

25. Budiansky, B, and O'Connell, RJ. Elastic moduli of dry and saturated cracked solids. *Int J Solids Struct* 1976; 12, 81–97.
26. Borgomano, J, Gallagher, A, Sun, C, and Fortin, J. An apparatus to measure elastic dispersion and attenuation using hydrostatic-and axial-stress oscillations under undrained conditions. *Rev Sci Instrum* 2020; 91(3): 034502.
27. Adelinet, M, Fortin, J, Guéguen, Y, Schubnel, A, and Geoffroy, L. Frequency and fluid effects on elastic properties of basalt: Experimental investigations. *Geophys Res Lett* 2010; 37(2): GL041660.
28. Pimienta, L, Borgomano, J, Fortin, J, and Guéguen, Y. Modelling the drained/undrained transition: Effect of the measuring method and the boundary conditions. *Geophys Prospect* 2016; 64: 1098–1111.
29. Cleary, MP. Elastic and dynamic response regimes of fluid-impregnated solids with diverse microstructures. *Int J Solids Struct* 1978; 14(10): 795–819.
30. Borgomano, J, Pimienta, L, Fortin, J, and Guéguen, Y. Dispersion and attenuation measurements of the elastic moduli of a dual-porosity limestone. *J Geophys Res: Solid Earth* 2017; 122(4): 2690–2711.
31. Pimienta, L, Fortin, J, and Guéguen, Y. Bulk modulus dispersion and attenuation in sandstones. *Geophysics* 2015; 80(2): D111–D127.
32. Borgomano, J, Pimienta, L, Fortin, J, and Guéguen, Y. Seismic dispersion and attenuation in fluid-saturated carbonate rocks: Effect of microstructure and pressure. *J Geophys Res: Solid Earth* 2019; 124(12): 12498–12522.
33. Yin, H, Borgomano, J, Wang, S, Tiennot, M, Fortin, J, and Guéguen, Y. Fluid substitution and shear weakening in clay-bearing sandstone at seismic frequencies. *J Geophys Res: Solid Earth* 2019; 124(2): 1254–1272.
34. Adelinet, M, Fortin, J, and Guéguen, Y. Dispersion of elastic moduli in a porous-cracked rock: Theoretical predictions for squirt-flow. *Tectonophysics* 2011; 503(1–2): 173–181
35. Fortin, J, Pimienta, L, Guéguen, Y, Schubnel, A, David, EC, and Adelinet, M. Experimental results on the combined effects of frequency and pressure on the dispersion of elastic waves in porous rocks. *Leading Edge* 2015; 33(6): 648–654.
36. Regnet, JB, Robion, P, David, C, Fortin, J, Brigaud, B, and Yven, B. Acoustic and reservoir properties of microporous carbonate rocks: Implication of micrite particle size and morphology. *J Geophys Res: Solid Earth* 2015; 120(2): 790–811.
37. Chapman, S, Borgomano, J, Yin, H, Fortin, J, and Quintal, B. Forced oscillation measurements of seismic wave attenuation and stiffness moduli dispersion in glycerin-saturated Berea sandstone. *Geophys Prospect* 2019; 67: 956–968.